X-921-76-258
PREPRINT

NASA TM X- 71253

COMPUTER SIMULATION OF EARTHQUAKES

STEVEN C. COHEN

NOVEMBER 1976

GSFC

GODDARD SPACE FLIGHT CENTER
GREENBELT, MARYLAND

X-921-76-258
Preprint

COMPUTER SIMULATION OF EARTHQUAKES

Steven C. Cohen

Geodynamics Branch

November 1976

GODDARD SPACE FLIGHT CENTER
Greenbelt, Maryland

COMPUTER SIMULATION OF EARTHQUAKES

Steven C. Cohen

Geodynamics Branch

ABSTRACT

Two computer simulation models of earthquakes are studied for the dependence of the pattern of events on the model assumptions and input parameters. Both models are adaptations from the work of Dieterich (Dieterich, 1972), and represent the seismically active region by mechanical blocks which are connected to one another and to a driving plate. The blocks slide on a friction surface. In the first model we employ elastic forces and time independent friction to simulate main shock events. We find that the size, length, and time and place of event occurrence are influenced strongly by the magnitude and degree of homogeniety in the elastic and friction parameters of the fault region. For example, periodically reoccurring similar events are frequently observed in simulations with near homogeneous parameters along the fault, whereas, seismic gaps are a common feature of simulations employing large variations in the fault parameters. The second model incorporates viscoelastic forces and time-dependent friction to account for aftershock sequences. The periods between aftershock events increase with time and the aftershock region is confined to that which moved in the main event.

CONTENTS

ILLUSTRATIONS

ILLUSTRATIONS (Continued)

I. INTRODUCTION

In the absence of a general theory of motion along a fault there are at least five avenues of approach to understanding earthquake dynamics. These avenues include field investigations, laboratory experiments, simplified theoretical analyses, model building, and computer-numeric simulations. The present paper focuses on a computer simulation. There are several reasons why such simulations are attractive research tools. The first of these is time compression. Events spanning many decades, even centuries, can be simulated in a few seconds on a high speed computer. The second is convenience in investigating alternative hypotheses. All the conditions of the simulation are under the control of the progr mmer and the differing consequences of alternative assumptions are readily identified. The third attractive feature is the great detail with which the motion can be observed in the simulation. This can be a great aid in explaining the consequences of the motion. The major difficulty with computer simulations is the question of correspondence with "real world" phenomena. Highly idealized models, which are clear in conceptual detail, may not be adequate representations of naturally occurring situations. On the other hand complex simulations are limited by our lack of knowledge about naturally occurring conditions and by restrictions on computer speed and storage requirements. Furthermore, complex simulations may be so confusing in detail that they are uninstructive in basic causes and effects. In the present effort we are aiming primarily for physical clarity and have, therefore, used conceptually simple ideas and techniques.

Despite this limitation, much of the behavior exhibited by our simulator mimics natural behavior and certain observed natural phenomena find ready explanation through this technique.

Most simulators are based on the model of coupled massive blocks first introduced by Burridge and Knopoff (Burridge and Knopoff, 1967) and illustrated in Figure 1. In this model the fault is divided into coupled blocks which slide on a frictional surface. The coupling which corresponds to the elastic and viscous properties of the material is represented by various combinations of springs and dashpots. The blocks are driven through a coupling to a moving plate. The plate moves with a drift velocity, u, which is unaffected by the frictional resistance along the fault. The one-dimensional model of Burridge and Knopoff included ten blocks some with predominate elastic coupling to their neighbors and some with predominate Maxwell-viscous coupling. Dieterich (Dieterich, 1972) elaborated on the model by including fifty blocks and using the standard linear solid coupling shown in Figure 1. Otsuka (Otsuka, 1972) developed a two-dimensional simulator with elastic couplding, and Dieterich (Dieterich, 1973) reported on a three-dimensional, elastic coupling, simulator.

In the present work we will examine in more detail some one-dimensional simulators, primarily those due to Dieterich. We will examine, in particular, such questions as how the pattern of stress release in simulator earthquakes (SEQs) depends on the frictional characteristics of the fault and how simulator aftershock sequences depend on material properties.

II. ELASTIC MODEL

The simplest model that we have employed assumes perfect elastic coupling between a block and its nearest neighbors and to the driving plate. Consider the elastic forces acting on the ith block of Figure 1

$$F_i = K_i(x_{i+1} - x_i) + K_{i-1}(x_{i-1} - x_i) + K_i'(ut - x_i) \tag{1}$$

where u is the velocity of the driving plate, t is the time, x_{i+1}, x_{i-1}, and x_i are the displacements of the i + 1, i - 1, and ith blocks, K_i and K_{i-1} are the spring constants of the i and i - 1 th connecting springs and K_i' is the spring constant of the leaf spring connecting block i to the driving plate. To each block we also associate a static frictional strength, f_i^s, which resists motion. Once the pulling force overcomes the frictional resistance to motion the dynamics of the ith block is governed by the force equation

$$\begin{aligned} m_i\ddot{x}_i &= F_i - f_i^d \\ &= K_i(x_{i+1} - x_i) + K_{i-1}(x_{i-1} - x_i) + K_i'(ut - x_i) - f_i^d \end{aligned} \tag{2}$$

where m_i is the block mass and f_i^d is the dynamic friction force.

Consider now the situation with all blocks initially at rest and $F_i < f_i^s$ for each block. As time advances F_i increases due to the motion of the driving block and the consequential increase in the driving spring tension. We can associate with each block a time, t_i^0, at which time the block would first move if unaffected by the motion of any other block. Thus

$$t_i^0 = \frac{1}{u}\left[\frac{K_i}{K_i'}(x_i^0 - x_{i+1}^0) + \frac{K_{i-1}}{K_i'}(x_i^0 - x_{i-1}^0) + \frac{f_i^s}{K_i'}\right] \tag{3}$$

That block which has the minimum value of t_i^0 is the first to move. The subsequent motion of all blocks can be determined as follows: No block moves until $F_i = f_i^s$ for that block. At that time the block's initial acceleration is

$$\ddot{x}_i^0 = \frac{F_i^0 - f_i^d}{m_i} = \frac{f_i^s - f_i^d}{m_i} \tag{4}$$

The subsequent dynamics is dictated by Equation 2. Initially the block's acceleration is positive and its position and velocity increase. As the tension on the block is relieved by the sliding motion the acceleration decreases becoming negative for sufficient spring compression. The velocity begins to decrease and ultimately goes to zero at which point motion of that block terminates if $|F_i| < f_i^s$. It is evident from the preceeding equations, however, that the motion of one block will cause compression or expansion of the connecting springs to its neighbors. This can stimulate motion of the adjoining blocks thereby propagating the earthquake along the fault. Thus the motion along the fault is governed by a set of coupled dynamic equations of the form of Equation 2. Numeric techniques for solving such equations are well known and we need comment here only that the solution would be ambiguous if we did not impose some boundary condition of the end springs. In the simulations reported here we have assumed periodic boundary conditions for N blocks (N = 50 in most of our simulations).

Before continuing the discussion it is instructive to solve analytically the simple case in which only one block moves during an earthquake. We further assume $K_i = K_{i+1} = K_i'$ and take as initial conditions $x_i^0 = x_{i+1}^0 = \dot{x}_i^0 = 0$. Then

suppressing the subscript i

$$\ddot{x} + \frac{3K}{m} x = \frac{Kut - f^d}{m} \tag{5}$$

Since the velocity of the driving plate is very slow (~5 cm/yr) the quantity Kut is essentially unchanged during the motion and we let $t = t_0 = \text{constant}$. Thus the equations of motion becomes

$$\ddot{x} + \frac{3K}{m} x = \frac{Kut_0 - f^d}{m} ; \tag{6}$$

which has the simple solution

$$x = \frac{2}{3}\left(ut_0 - \frac{f^d}{K}\right) \sin^2 \sqrt{\frac{3K}{m}} \frac{(t - t_0)}{2} \tag{7}$$

But the condition for starting motion is $Kut_0 = f^s$ so that

$$x = \frac{2}{3}\frac{f^s}{K}(1 - a)\sin^2 \sqrt{\frac{3K}{m}} \frac{t}{2} ; \; a = \frac{f^d}{f^s} \tag{8}$$

We take note of several easily derived consequences. First the total displacement of block i due to this event is

$$x_{max} = \frac{2}{3}\frac{f^s}{K}(1 - a) \tag{9}$$

while the duration of the event is

$$t_{max} - t_0 = \sqrt{\frac{m}{3K}}\,\pi \tag{10}$$

Notice that the duration of the single block event depends only on the mass of the block and the spring constant and is unaffected by the friction parameters. The

peak velocity is

$$\dot{x}_{max} = \frac{(f^s - f^d)}{\sqrt{3Km}} \tag{11}$$

The typical time scale for re-occurrence of motion in this block is

$$\Delta T \sim \frac{f^s - f^d}{Ku} \tag{12}$$

The initial force on block i was Kut_0. The final force is $\sim K(ut_0 - 3x_{max})$. Thus the change in the stress force, ΔF, is

$$\Delta F_i = 3Kx_{max} = 2(f^s - f^d) \tag{13}$$

and

$$\frac{\Delta F_i}{F_i^0} = 2(1 - a) \tag{14}$$

The stress force rise in the adjacent block (e.g., ΔF_{i+1}) is

$$\Delta F_{i+1} = Kx_{max} = \frac{2}{3}(f^s - f^d) \tag{15}$$

$$\frac{\Delta F_{i+1}}{F_{i+1}^0} = \frac{2}{3}(1 - a) \tag{16}$$

Notice that the fractional stress changes depend only on the ratio of dynamic to static friction, independent of other material properties. If, for example, a = 0.8, there is a forty percent drop in the stress of the ith block due to this event and a thirteen percent increase in the stress of its neighbors. If this additional stress rise were sufficient to overcome the frictional strength of the neighbors these blocks would have been stimulated into motion. Furthermore, the absolute change in the stress force as a result of the earthquake is determined by twice the

difference between the static and dynamic frictional strengths, again independent of other material parameters.

III. VISCOELASTIC MODEL WITH TIME-DEPENDENT FRICTION

The elastic model which we discussed in the last section generates simulations which have many features common to naturally occurring events. These features include the slow accumulation of tectonic stress and its rapid release by stick-slip sliding in earthquakes, the existence of seismic gaps in areas on high frictional and elastic constant variability, and the gradual propagation of a secession of earthquake events through regions of relative uniform properties. Events of varying magnitude, ground displacements, and volume are generated. Nevertheless there are a number of important phenomena which cannot be simulated with this model. Foremost among these are aftershock sequences. In order to generate aftershocks we assume some mechanism for the rapid recovery of all or part of the stress released by the main shock is necessary. The tectonic forces represented by the slowly stretching elastic springs build too slowly to provide an aftershock mechanism. By contrast, Burridge and Knopoff (Burridge and Knopoff, 1967) showed that viscous creep following an earthquake can redistribute stress in a manner which produces aftershocks. Dieterich (Dieterich, 1972) proposed partial stress recovery due to viscoelasticity in a region which slides during an earthquake then remains locked while the viscous forces adjust to the displacement. When coupled with a post-earthquake weakening of the fault

frictional strength this mechanism will also generate aftershock sequences. We now elaborate on this model.

Consider the same mechanical blocks as in the previous section. Now, however, instead of having coupling by simple elastic springs, the coupling is a parallel combination of elastic and Maxwellian elements as shown in insert b of Figure 1. Assuming that the blocks are not moving and that the driving plate velocity is still u. The viscoelastic force equation is

$$\begin{aligned} F_i = {} & G_i e^{-(t - t_{i+})/\tau_i} + G_{i-1} e^{-(t - t_{i-})/\tau_{i-1}} + G'_i e^{-(t - t_i)/\tau'_i} \\ & + K_i(x_{i+1} - x_i)(1 - e^{-(t - t_{i+})/\tau_i}) + K_{i-1}(x_{i-1} - x_i)(1 - e^{-(t - t_{i-})/\tau_{i-1}}) \\ & + K'_{2_i} u\tau'_i(1 - e^{-(t - t_i)/\tau'_i}) + K'_i u(t - t_i e^{-(t - t_i)/\tau'_i}) \\ & - K'_i x_i(1 - e^{-(t - t_i)/\tau'_i}) \end{aligned} \tag{17}$$

In the preceeding equation we have introduced the following symbols:

G_i = force on spring i at time t_{i+}

G_{i-1} = force on spring i - 1 at time t_{i-}

G_0 = force on spring i' at time t_i

t_{i+} = last time block i or block i + 1 moved

t_{i-} = last time block i or block i - 1 moved

t_i = last time block i moved.

The tau's (τ) are the relaxation times of the viscoelastic system. The condition for the onset on a simulation earthquake is

$$F_i(t) = f_i^s(t) \tag{18}$$

where the static frictional strength $f_i^s(t)$, is also a weak function of time increasing slowly from some minimum value immediately following cessation of block motion. Equation 17 is a transcendental equation for which can be solved by any of several numeric techniques. The acceleration and de-acceleration occurring during an earthquake occur on a time scale much faster than the viscous response time hence we can ignore viscous properties during the earthquake and write the following equation of motion

$$\begin{aligned} m\ddot{x}_i = & \left[K_i(x_{i+1} - x_i) + K_{i-1}(x_{i-1} - x_i) + K_i'(ut - x_i)\right] \\ & + \left[K_{2_i}((x_{i+1} - x_i) - (x_{i+1}^0 - x_i^0)) + K_{2_{i-1}}((x_{i-1} - x_i) - (x_{i-1}^0 - x_i^0))\right. \\ & \left. + K_{2_i}'((ut - x_i) - (ut_0 - x_i^0))\right] + [\mathfrak{F}_i^0 + \mathfrak{F}_{i+}^0 + \mathfrak{F}_i^{0'}] - f_i^d \end{aligned} \quad (19)$$

In this equation the first bracketed quantity represents the elastic force due to the stretching of the purely elastic element of Figure 1c. The second and third bracketed quantities represent the forces on the Maxwell elements. The second bracket gives the change in the elastic force due to stretching or compression of Maxwell elements springs from their position at beginning of simulation earthquake. The third bracket gives the force prior to this stretching or compression. This model has two key elements: the viscoelasticity is responsible for a partial recovery of the stress drop occurring during an earthquake event and the time dependent friction is responsible for a weakening of the fault strength. The model operates as follows. Assume initially (for simplicity only) that all elastic and Maxwell elements are relaxed, that there is no stress acting on any of the blocks. As in the purely elastic model, stress accumulates with the drift of the driving

plate until one block is stressed beyond its frictional strength and begins to slide. The subsequent motion may involve one or more blocks depending on the frictional strength of the other blocks. The motion of the blocks results in a stress drop whose magnitude is determined by the sum of the products of the spring constants and the change in spring stretch. This is all similar to the pure elastic case. Now, however, while the blocks remain fixed following the simulated earthquake the viscous dashpots tend to adjust to relax the stretch or compression in the Maxwell element springs. Consider the primed coupling element which has undergone a reduction in the spring stretch ΔL. The resultant stress drop is $(K' + K'_2)\,\Delta L$. If the Maxwell element dashpot has sufficient time to relax the change in the stretch of the K'_2 spring, then the final stress drop following viscous adjustment is $K'\Delta L$. Thus the fractional stress recovery of the original stress drop is $K'_2/(K' + K'_2)$. Assume, for illustrative purposes that $K'_2 = 3K'$, then seventy five percent of the original stress drop during a simulation earthquake is recovered during the subsequent stress rise due to viscous adjustment. If the frictional strength of the fault in this region is sufficiently reduced after the earthquake compared to the pre-earthquake level and if the viscous response is sufficiently rapid, then an aftershock will be generated. The process may be repeated many times. The reduction in frictional strength along the displaced portion of the fault is a consequence of the finite time required to heal the break subsequent to the slippage. This model uses a friction strength which rises logarithmically with time since the last slip. The time scale for the aftershocks is

usually of the same order as the viscous relaxation time. We will present illustrations of these aftershock sequences in the following section. We should emphasize that this aftershock theory is just one of several alternative treatments of the aftershock problem. Subsequent papers will deal with computer simulations employing other theoretical models.

IV. RESULTS

We now discuss the results of simulations using the models discussed in the previous sections. We first consider the simple case of purely elastic coupling between the blocks and the driving plate. Figure 2a shows block acceleration, velocity, and displacement versus time for typical small two block event. This SEQ was initiated when the elastic forces acting on block 44 overcame the static frictional strength of the block. The block begins to move with a peak acceleration 11 cm/sec^2.* As this block slides to the right and begins to relax the force acting on it, additional force is applied to blocks 43 and 45 by the compression and extension of the i = 43 and i = 44 springs. At ~7 seconds after the initiation of the event, the force on block 43 has reached the frictional strength limit of that block and it too begins to move to the right. As both blocks continue to slide to the right additional force is applied to blocks 42 and 45. Nevertheless these blocks remain unmoved as even the additional stress due to the motion of blocks

*The acceleration, velocity, displacement, and time axis shown on Figure 2 are scaled by the independent parameters f, K, and m. Thus, for example, the forty second time scale of Figure 2 is arbitrary to the extent that independent parameters can be changed. See the Appendix for the scale relationships.

44 and 43 is insufficient to overcome the frictional strengths. The moving blocks continue to deaccelerate until they come to rest at ~34 and 39 seconds after the initiation of the event. The force conditions on the fault preceeding and following this SEQ are also shown in Figure 2. Notice the stress relaxation in the moved blocks and the stress buildup in the adjacent unmoved blocks. In the case where the frictional and elastic properties of the fault region vary only slightly from block to block, this predisposes this unmoved border region to motion in a subsequent SEQ. By this mechanism the location of SEQ's propagates down the entire fault leaving few, if any, seismic gaps. We can see this more clearly in an event plot as shown in Figure 3. In this plot each line summarizes pertinent information concerning one SEQ. The first column gives the event number, the second the time of occurrence of the SEQ. The third column of fifty spaces represents the fifty blocks of the fault used in our simulations. Motion of a particular block during the event is indicated by an X; otherwise the space is left blank. Thus in event 316 at time $\simeq 5.147 \times 10^{10}$ seconds, blocks 6 through 9 moved and all other blocks remained stationary. The fourth column gives the block number of the first block to move in the event, and the fifth column tells the total number of blocks displaced in the SEQ. Figure 3 is an event plot for which all $K_i' = 1 \times 10^{17}$ dyne/cm, $K_i = K_i'/2$, and the f_i^s were in the range $(1.95\text{-}2.05) \times 10^{20}$ dynes. All the blocks have an equal mass of 2.8×10^{28} grams. Notice that in this case there is a cycle of similar events which tend to repeat themselves. Although there is no true periodicity of events, there is an approximate characteristic

time interval of about 2.5×10^8 seconds during which almost all blocks along the fault move at least once.

By contrast to this case where the elastic and frictional properties vary only slightly from block to block, we now consider a case, Figure 4, in which the friction is allowed to vary randomly from 1×10^{20} to 3×10^{20} dynes. In this case there is considerably more scatter in the location of SEQ's.

Figures 5 and 6 show two other cases of some interest. In Figure 5 the frictional strength varies smoothly from a minimum value of about 1×10^{20} dynes at blocks 1 and 50 to a maximum value near 3×10^{20} dynes in the middle of the fault. The function chosen to represent this variation is $f_i^s = 3.16 \times 10^{20} \exp(-(i - 25.5)/24.5)^2 - 0.16 \times 10^{20}$ (dynes). Because of the symmetry of the fault equal simultaneous events occur on the right and left sides of the figure. Two distinct patterns are observed. In the early stages of the simulation the pattern of SEQ events traces out the friction curve. The weaker elements move frequently with small slippages while the stronger elements are more resistant to being displaced. Gradually, however, the pattern evolves into one in which large sections of the fault move in discrete steps separated by intervals of little activity in those sections. The reoccurrence time between the large events decreases with time while the number of blocks involved increases. After the largest of these events has been completed much of the tension in these sections of the fault has been relieved, and the earlier pattern of tracing out the friction

curve is repeated. This behavior is characteristic of a situation in which the fault goes through a charge-discharge cycle. During the charging phase stress gradually accumulates and the small events which do occur only partially relieve the mounting stress. Finally a large event or events discharge most of the accumulated stress after which the cycle begins anew.

In Figure 6 the friction is, as in Figures 3 and 4, randomly distributed, but now the limits on the random number generator are $0\text{-}1 \times 10^{20}$ dynes. The particular distribution used is shown on the figure. We notice in Figure 6 that the weak elements move frequently, often in single block events.

A critical factor in determining the number of blocks that move in a given SEQ is the relative magnitudes of the connecting and leaf springs. Larger values of the leaf spring constants (relative to that of the connecting springs) favor events with a large number of blocks moving. The explanation is simply that with the larger leaf spring constant the tension between the moving plate and the associated connected block can be relieved with a relatively small displacement. This small displacement coupled to the weaker spring constant of the connecting spring is less likely to induce motion in the adjacent block than it would if the situation were reversed.

Three examples of simulations using the viscoelastic model are shown in Figure 7. The effect of the longer time constant in reducing the number of aftershocks and in increasing their inter-event period is obvious. Results generated

by the viscoelastic model are very sensitive to the relative values of the elastic and viscous parameters. We have performed simulations with many combinations of these parameters in the ranges 10^{16} dynes $\leq K' \leq 10^{18}$ dynes, $0.1 \leq \frac{K'}{K} \leq 10$, $1.5 \leq \frac{K_2}{K}$ and $\frac{K_2'}{K'} \leq 5$, $10 \leq \tau'$ and $\tau \leq 10^4$, $0 < f^s \leq 3 \times 10^{20}$ dynes and $0 < \frac{f^d}{f^s} \leq 0.99$.

Several general observations can be made.

1. For simulations in which $K = K'$ and $K_2 = K_2'$ the number of blocks moving during a typical event rises as the system advances from an unstressed to highly stressed state. Eventually a condition is reached when a high fraction of the simulation events involve all or nearly all blocks. This condition is influenced to some extent by the choice of periodic boundary conditions.

2. Conditions favoring a large number of aftershocks include small viscoelastic response times and larger values of K_2' with respect to K'. The former condition assures that the full effects of the viscoelastic stress recovery will be rapid compared to the time for appreciable rise in the frictional strength. The second condition implies that an appreciable portion of the initial stress drop during the SEQ is subsequently reduced so that the post-SEQ stress level approaches the pre-SEQ level.

3. The aftershocks tend to have smaller displacements than the main shock. This is consistent with the trend observed in nature and with the fact that

only a partial stress recovery occurs. It is not true however, that there is a monotonic decrease in the average displacement with aftershock number. The exact nature of the aftershock displacements depends in a complicated manner on the frictional characteristics, viscoelastic parameters, and number of blocks involved in the event.

4. The mean time between aftershocks tends to increase with time. For some simulations the time interval between the main and first aftershock is the minimum time interval between events in a sequence. In other cases the minimum time interval occurs between the first and second aftershocks. In either case there is a subsequent trend toward increasing periods between aftershocks provided aftershocks with a common epicentral block are considered. For aftershocks with different epicentral blocks there may be a super-position of several sequences, each involving its own epicentral block. Alternatively, the behavior may be more complicated. Some of the simulated aftershock sequences show a logarithmic increase in the number of aftershocks with time, consistent with Omori's (Omori, 1894) observation of a $(a + bt)^{-1}$ dependence of aftershock frequency on time following the main shock. In other cases there are considerable deviations from this simple time dependence.

5. The aftershock region is generally confined to the region of the main shock. The number of blocks displaced in an aftershock is less than or sometimes equal to the number displaced in the main event.

V. CONCLUSIONS

In this paper we have begun our examination of various numerical simulators of earthquakes. We have focused attention on two theoretically simple models, one employing elastic forces and time-independent friction, the other employing viscoelastic forces and time-dependent friction. Our central conclusions are as follows:

1. When the elastic and frictional parameters are nearly uniform from block to block the SEQ's are characterized by a propagation of successive events down the fault. Conversely, seismic gaps are more likely to occur when there are large variations in the elastic or frictional parameters.

2. The periodic reoccurrence of similar SEQ events is frequently observed in cases where the parameters of the fault and the blocks are nearly homogeneous from location to location. The reoccurrence time is determined primarily by the difference between the static and dynamic friction and by the elastic constants of the springs.

3. Simulator events involving large displacements tend to involve the motion of several blocks. The simultaneous motion of adjacent blocks lessens the displacement restricting elastic forces between blocks.

4. Frictionally weak elements tend to move frequently with concomitant small average displacements.

5. As the ratio, $\frac{K'}{K}$, of the elastic driving force constant to connecting force constant increases, the length of the average SEQ event decreases.

6. In the viscoelastic model the aftershocks exhibit several characteristic features:

   a. the period between aftershocks increases with time following the main event,

   b. the magnitudes and block displacements of the aftershocks are less than that of the main shock. However, there is no consistent decrease in aftershock magnitude with time,

   c. the aftershocks are confined to the region of the main event. Fewer, or at most the same, number of blocks are involved in aftershocks.

7. The occurrence of aftershocks in the viscoelastic model is enhanced by short viscoelastic time constant, τ, and by large values of the ratio $\frac{K_2'}{K}$.

Several features concerning numerical simulators await further investigation. These features include, among others, the exploration of alternative earthquake theories particularly with respect to fault friction instability and aftershock occurrence. Also deserving examination in the correlation among the input and output parameters of the model. For example, King (King, 1975) has observed in his mechanical models the statistically valid relationship: log (Energy released)

$= A + B \log(N\bar{d})$ where N is the number of blocks involved in the event, $\bar{d}$ is the average block displacement, and $B \simeq 1$. We have observed a similar correlation in our numerical simulations. Finally a detailed examination of the importance of boundary conditions and geometry and topology in two and three dimensional models also awaits further discussion. We hope to address some of these questions in subsequent papers.

REFERENCES

Burridge, R. and L. Knopoff (1967). Model and theoretical seismology, Bull. Seism. Soc. Am. 57, 341-371.

Dieterich, J. H. (1972). Time-dependent friction as a possible mechanism for aftershocks, J. Geophys. Res. 77, 3771-3781.

Dieterich, J. H. (1973). A deterministic near-field source model, Proc. Fifth World Conf. Earthquake Eng., Rome.

King, C. Y. (1975). Model seismicity and faulting parameters, Bull. Seism. Soc. Am. 65, 245-259.

Omori, F. (1894). On the aftershocks of earthquake, J. Coll. Science Imp. Univ. Tokyo 7, 133-152.

Otsuka, M. (1972). A simulation of earthquake occurrence, Phys. Earth Planet Interiors 6, 311-315.

FIGURE CAPTIONS

Figure 1. Mechanical block representation of fault. Each block which rests on the friction surface is coupled to nearest neighbors and to the driving plate which moves to the right with velocity u. (a) elastic coupling element - perfect spring with spring constant K. (b) viscoelastic coupling with spring constants K and K_2 and dashpot viscosity η.

Figure 2. Example of a two block SEQ. The displacement velocity, and acceleration of blocks 43 and 44 are shown as a function of time. This SEQ occurred early in a simulation when the pre-SEQ stresses on blocks 42-45 were equal. After the SEQ the stress on the moved blocks has been reduced while the stress on the adjacent unmoved blocks has risen.

Figure 3. Event plot for simple elastic force model with $K_i' = 1 \times 10^{17}$ dyne/cm, $K_i = 5 \times 10^{16}$ dyne/cm and f_i^s randomly distributed in range $(2 \pm 0.5) \times 10^{20}$ dyne.

Figure 4. Event plot for simple elastic force model with K_i' and K_i as in Figure 3 but f_i^s randomly distributed in range $(2 \pm 1) \times 10^{20}$ dyne.

Figure 5. Event plot for simple elastic force model with K_i' and K_i as in Figures 3 and 4 and $f_i^s = 3.16 \times 10^{20} \exp(-(i - 25.5)/24.5)^2 - 0.16 \times 10^{20}$ (dynes).

FIGURE CAPTIONS (Continued)

Figure 6. Event plot for simple elastic force model with K_i' and K_i as in Figures 3-5 but f_i^s randomly distributed in range $0 < f_i^s < 1 \times 10^{20}$ dyne.

Figure 7. Event plot for viscoelastic force model with time dependent friction. The parameters of the simulation are $K_i' = 1 \times 10^{18}$, $K_{2_i}' = 3K_i$, $K_i = 1 \times 10^{17}$, $K_{2_i} = 3K_i$, 1×10^{20} dyne $< f_i^s(t_0) < 3 \times 10^{20}$ dyne, $f_i^d = 0.98 f_i^s(t_0)$, $f_i^s(t) \approx f_i^s(t_0)[1 + 0.021 \log(1 + t - t_0)]$.

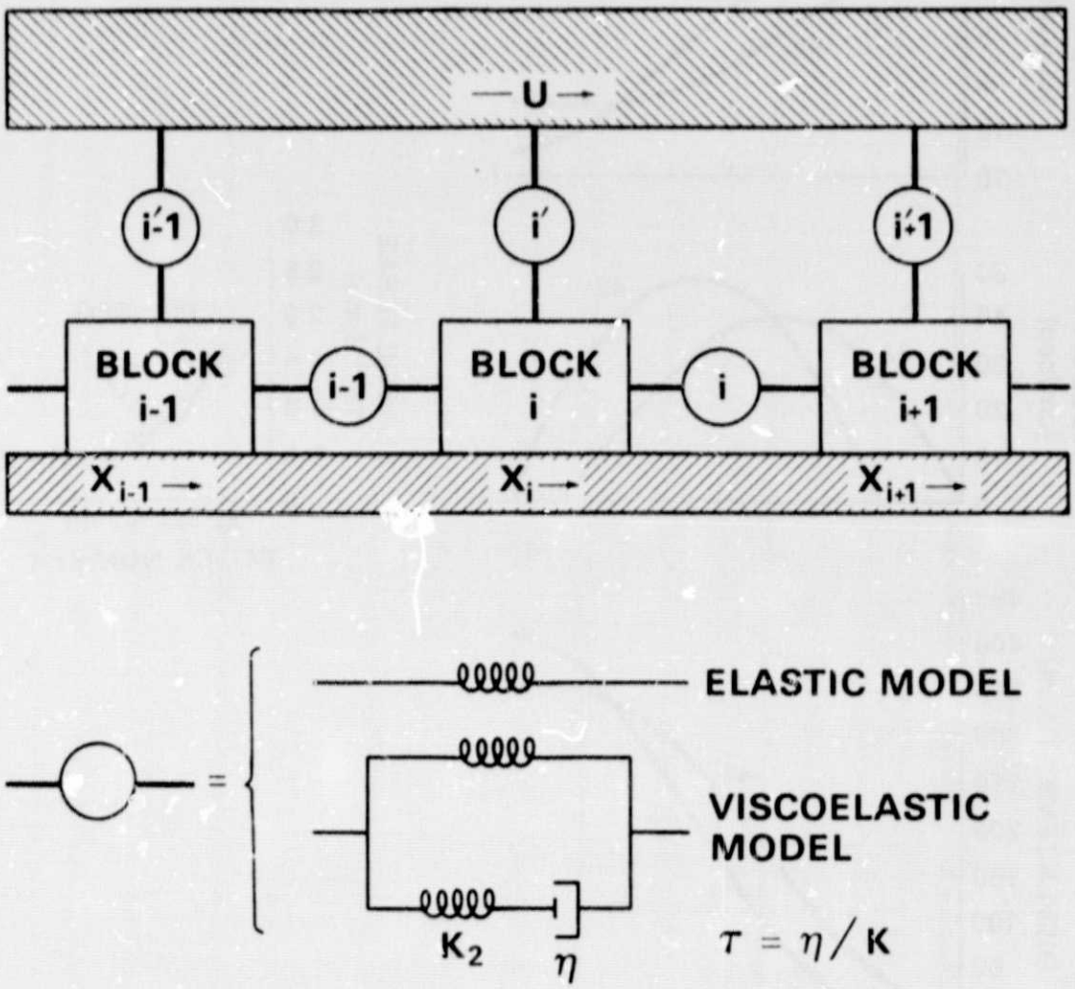

Figure 1. Mechanical block representation of fault. Each block which rests on the friction surface is coupled to nearest neighbors and to the driving plate which moves to the right with velocity u. (a) elastic coupling element - perfect spring with spring constant K. (b) viscoelastic coupling with spring constants K and K_2 and dashpot viscosity η.

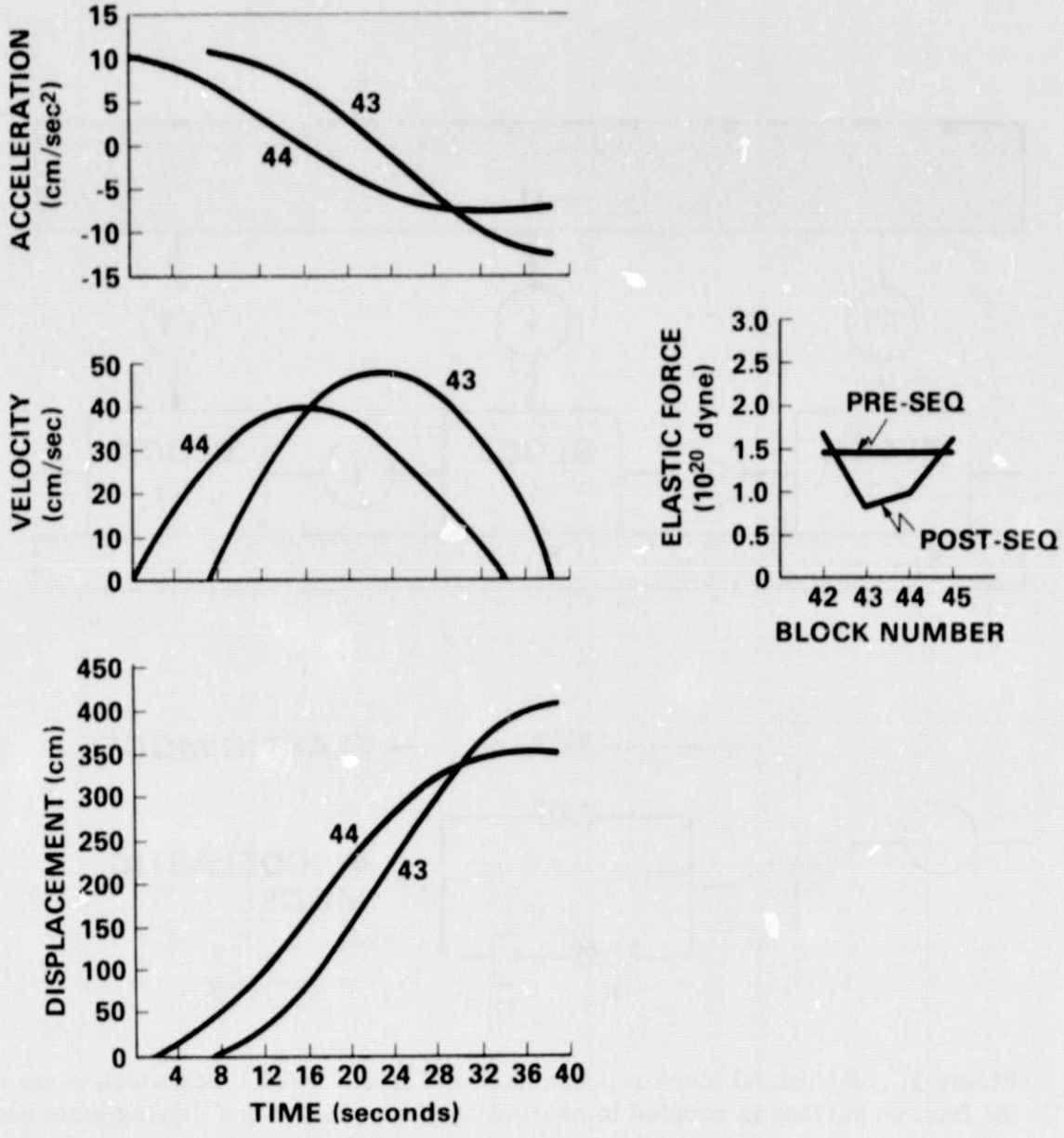

Figure 2. Example of a two block SEQ. The displacement velocity, and acceleration of blocks 43 and 44 are shown as a function of time. This SEQ occurred early in a simulation when the pre-SEQ stresses on blocks 42-45 were equal. After the SEQ the stress on the moved blocks has been reduced while the stress on the adjacent unmoved blocks has risen.

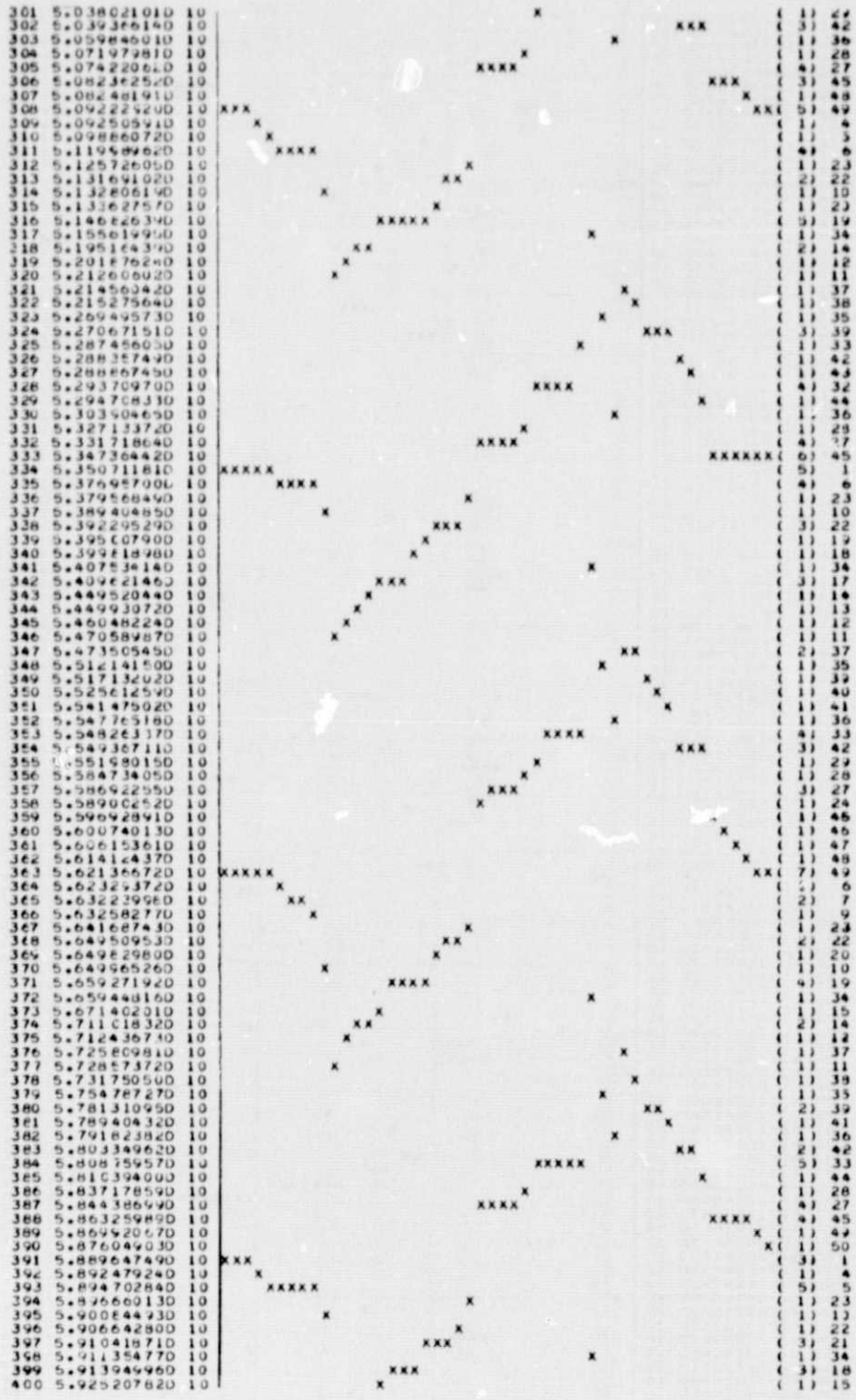

Figure 3. Event plot for simple elastic force model with $K_i' = 1 \times 10^{17}$ dyne/cm, $K_i = 5 \times 10^{16}$ dyne/cm and f_i^s randomly distributed in range $(2 \pm 0.05) \times 10^{20}$ dyne.

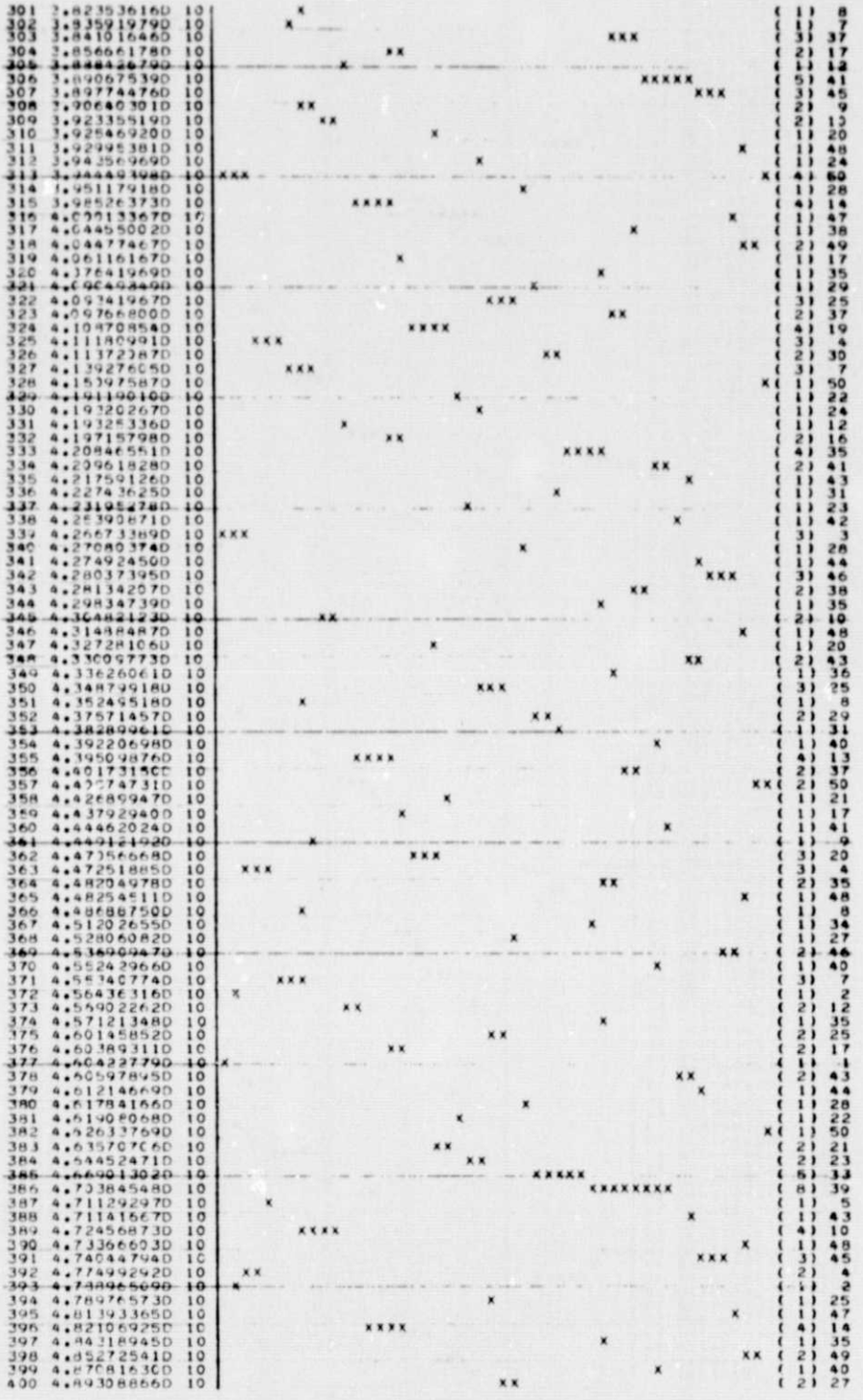

Figure 4. Event plot for simple elastic force model with K_i' and K_i as in Figure 3 but f_i^s randomly distributed in range $(2 \pm 1) \times 10^{20}$ dyne.

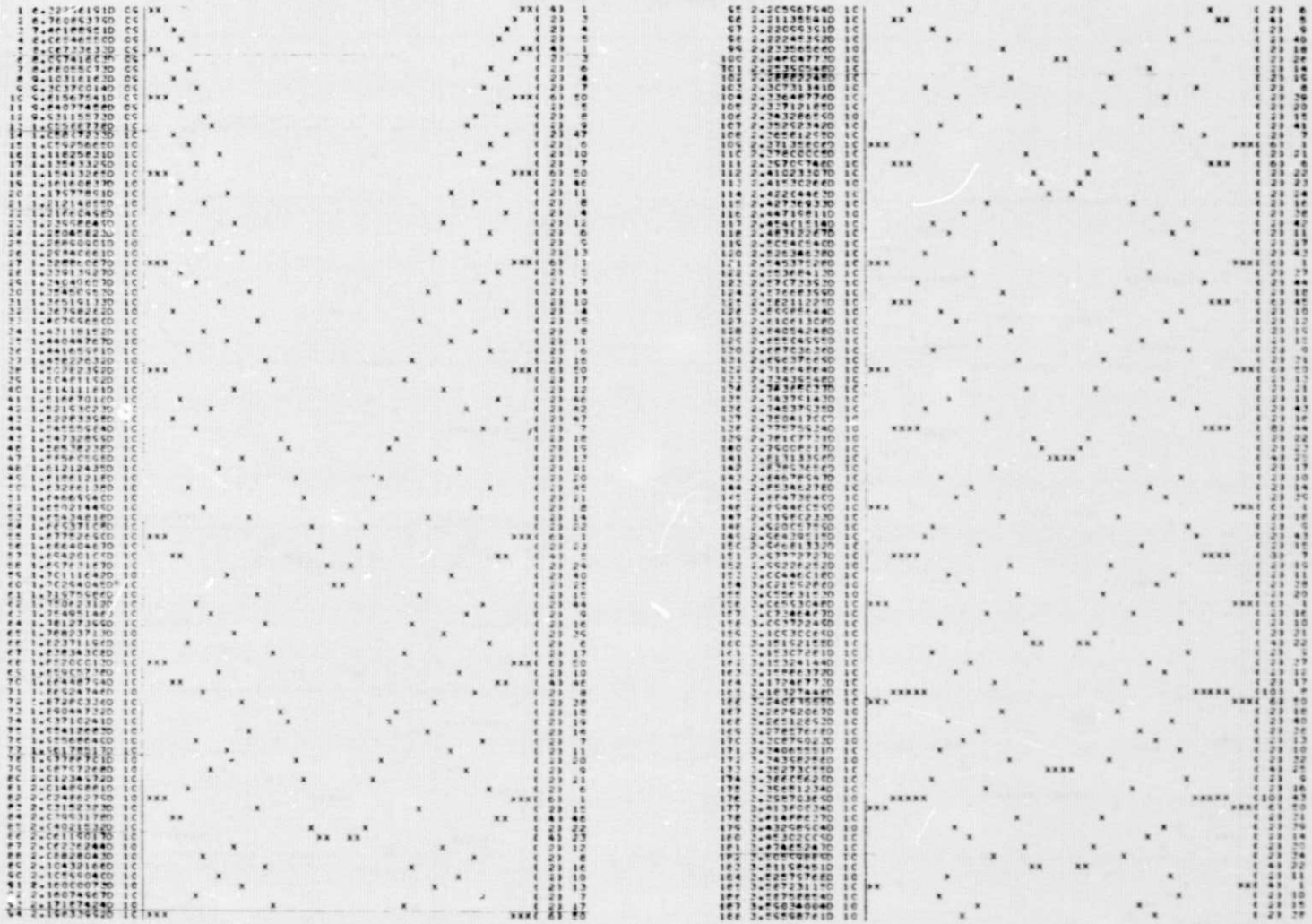

Figure 5. Event plot for simple elastic force model with K_i' and K_i as in Figures 3 and 4 and $f_i^s = 3.16 \times 10^{20} \exp(-(i - 25.5)/24.5)^2 - 0.16 \times 10^{20}$ (dynes).

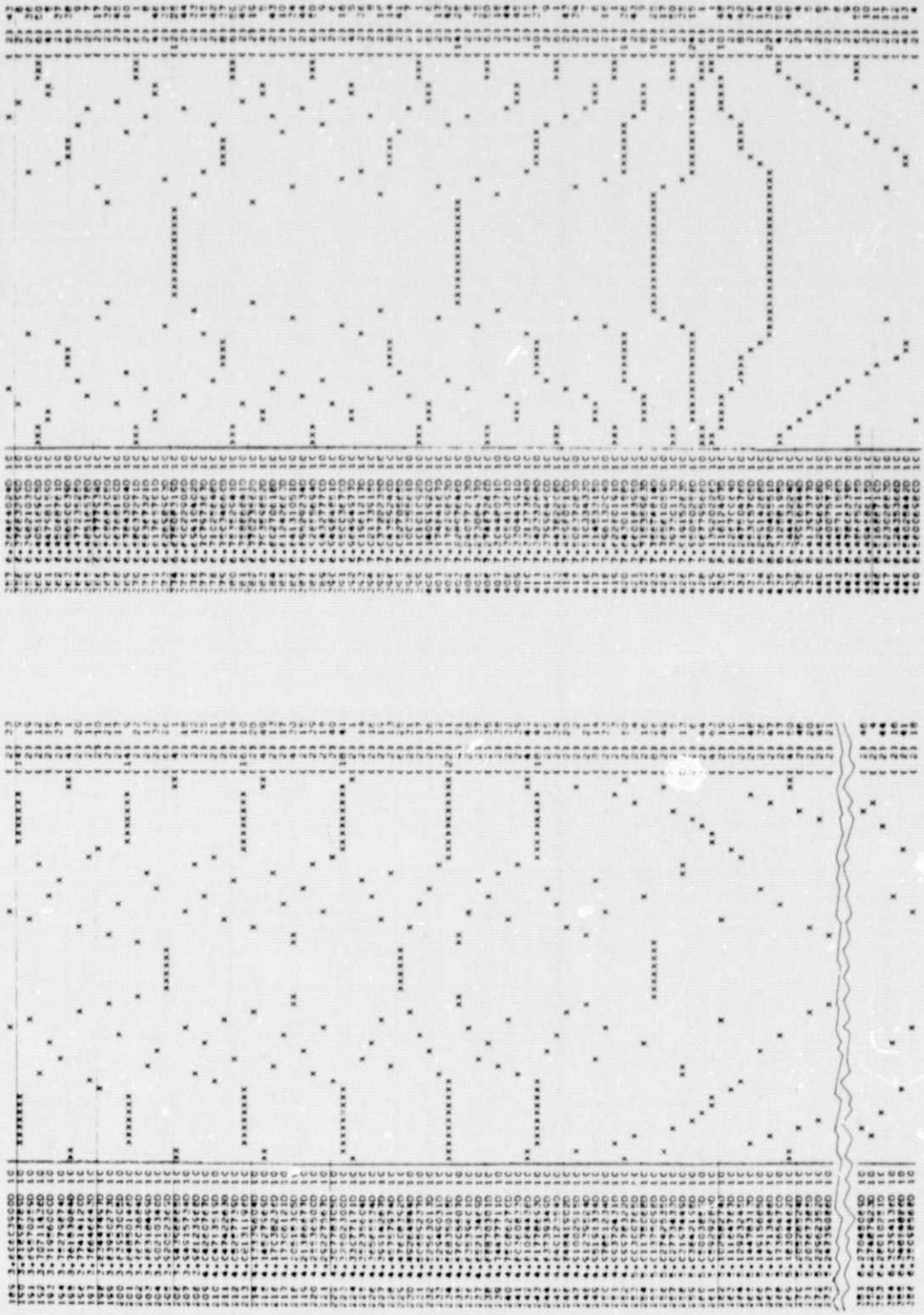

Figure 5. (Continued)

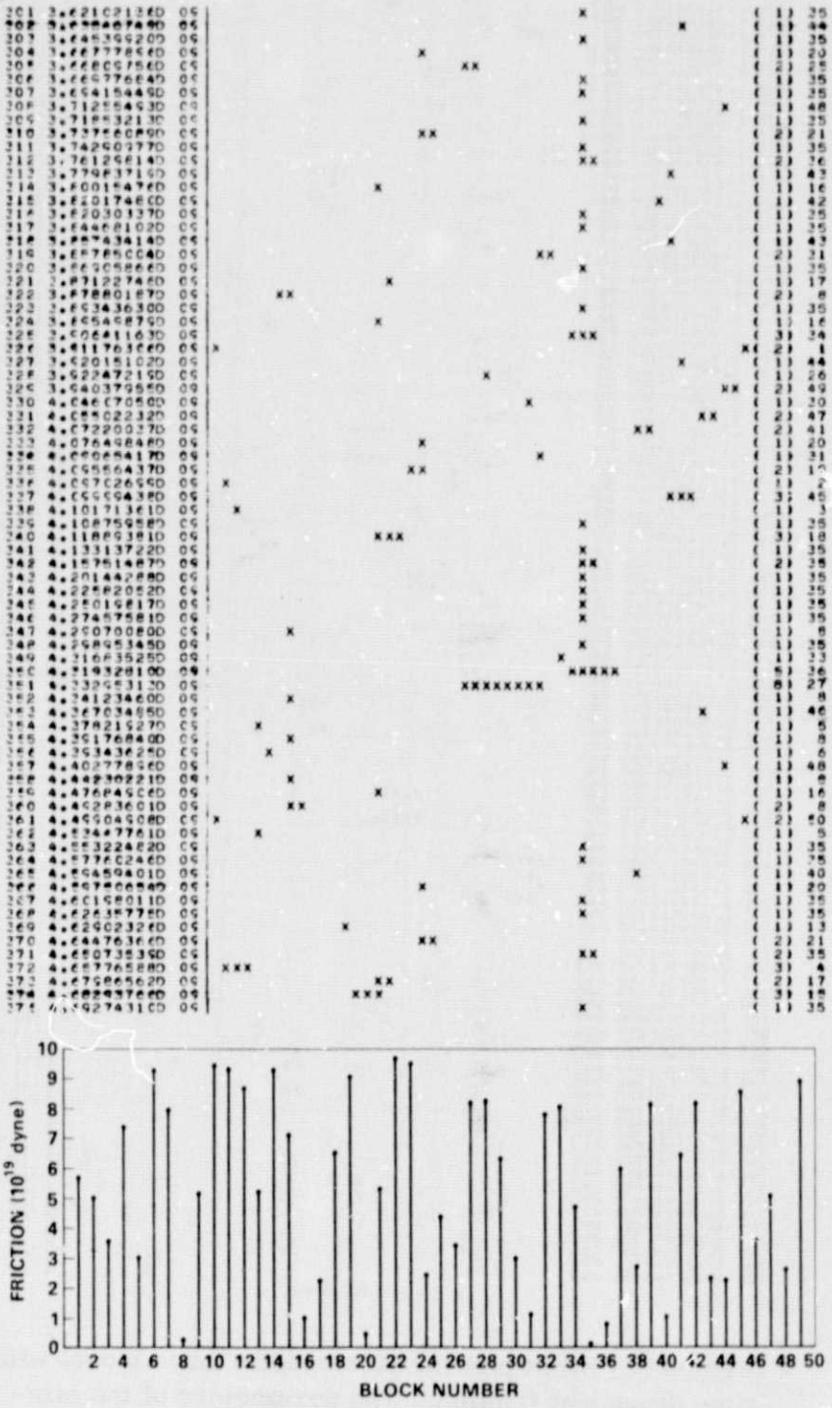

Figure 6. Event plot for simple elastic force model with K_i' and K_i as in Figures 3-5 but f_i^s randomly distributed in range $0 < f_i^s < 1 \times 10^{20}$ dyne.

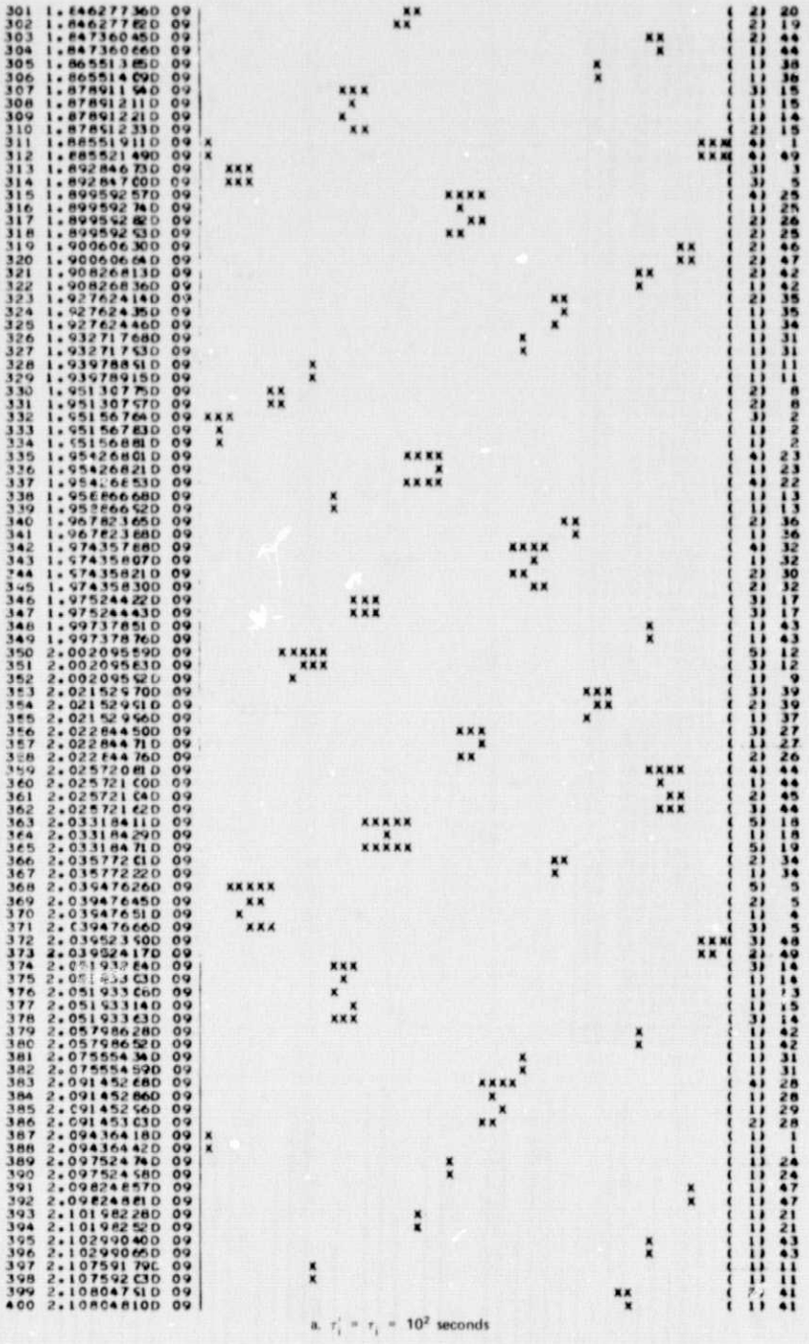

a. $\tau_i' = \tau_i = 10^2$ seconds

Figure 7. Event plot for viscoelastic force model with time dependent friction. The parameters of the simulation are $K_i' = 1 \times 10^{18}$, $K_{2i}' = 3K_i$, $K_i = 1 \times 10^{17}$, $K_{2i} = 3K_i$, 1×10^{20} dyne $< f_i^s(t_0) < 3 \times 10^{20}$ dyne, $f_i^d = 0.98\, f_i^s(t_0)$, $f_i^s(t) = f_i^s(t_0)\,[1 + 0.021 \log(1 + t - t_0)]$.

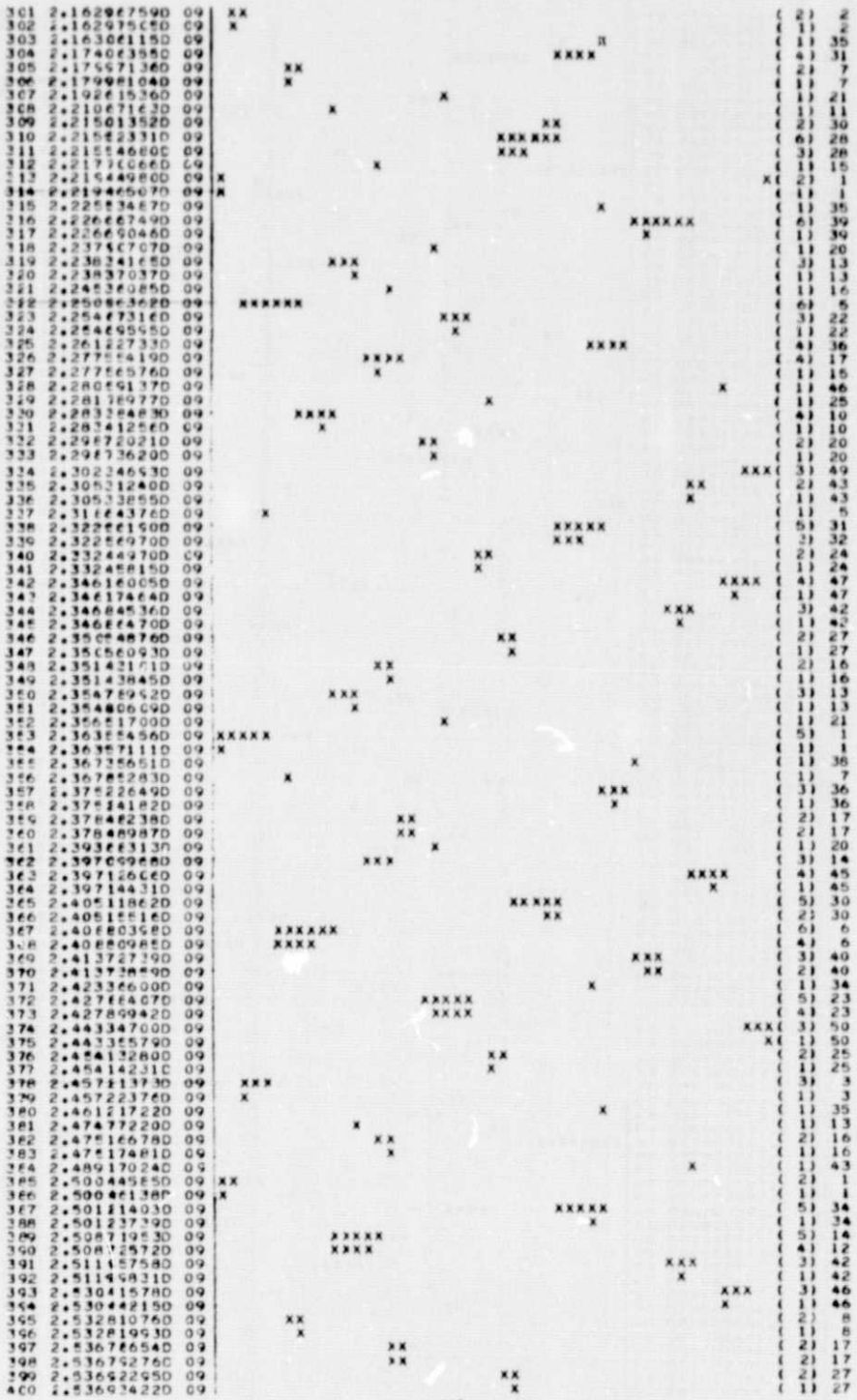

b. $r_i' = r_i = 10^3$ seconds

Figure 7. (Continued)

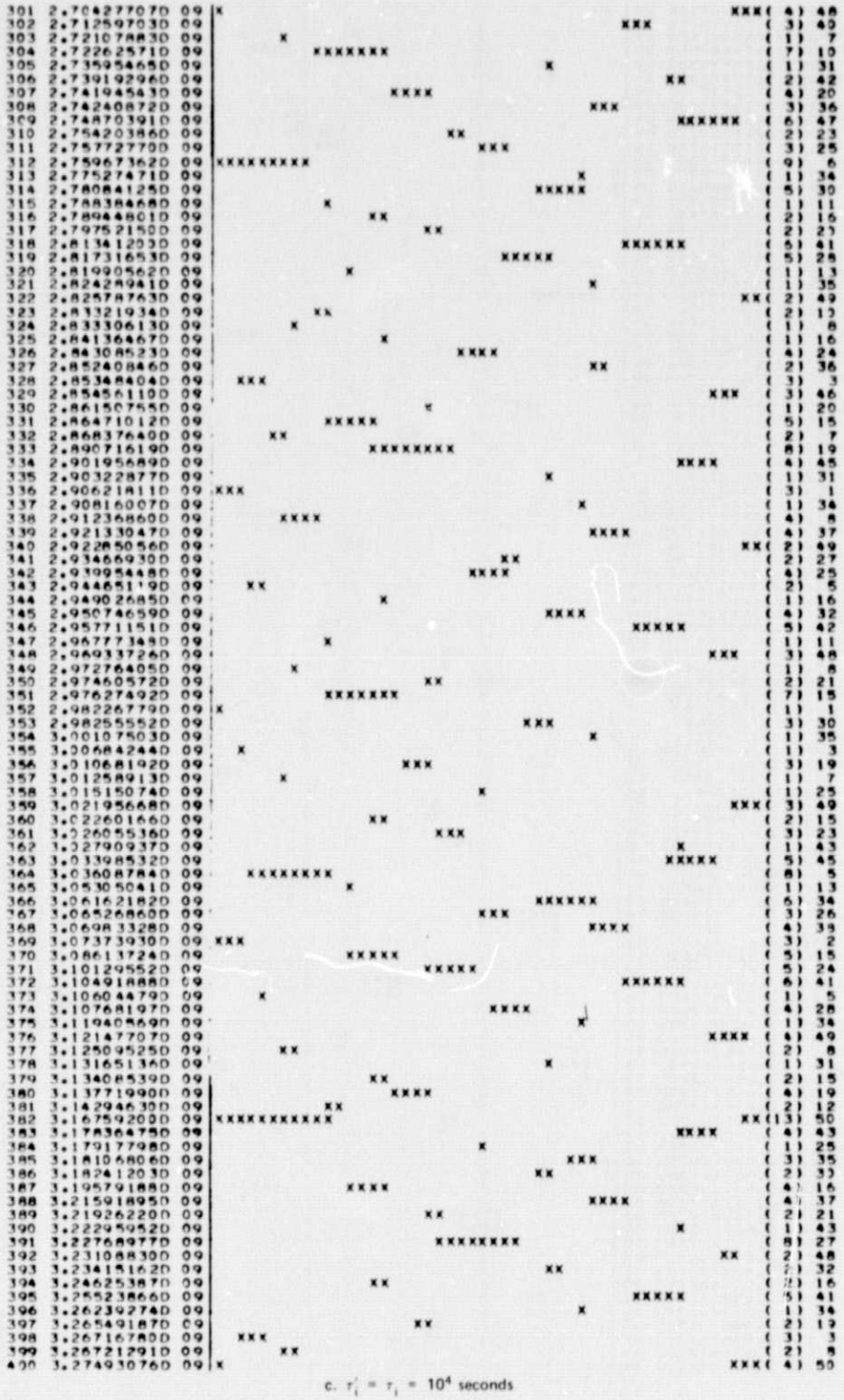

c. $\tau_i' = \tau_i = 10^4$ seconds

Figure 7. (Continued)

APPENDIX

SCALING LAWS

The results of a simulation can be scaled according to the following relations derived from Equation 2.

Given: the results from a simulation performed with independent parameters

f', K', m'

Define:

$$f = Bf' \tag{A.1}$$

$$K = CK' \tag{A.2}$$

$$m = Dm' \tag{A.3}$$

Then:

$$x = \frac{B}{C} x' \tag{A.4}$$

$$\dot{x} = \sqrt{\frac{B}{CD}}\, \dot{x}' \tag{A.5}$$

$$\ddot{x} = \frac{B}{D} \ddot{x}' \tag{A.6}$$

$$t_0 = \sqrt{\frac{D}{C}}\, t_0' \tag{A.7}$$

$$\Delta t = \frac{B}{C} \Delta t' \tag{A.8}$$

where $\Delta t'$ is a time interval associated with block motion. We have assumed $\Delta t' \ll t_0'$.